

Cite this: DOI: 10.1039/c2cp41578j

www.rsc.org/pccp

PAPER

Electronic transport and mechanical stability of carboxyl linked single-molecule junctions

Seokhoon Ahn,^a Sriharsha V. Aradhya,^b Rebekka S. Klausen,^a Brian Capozzi,^b Xavier Roy,^a Michael L. Steigerwald,^a Colin Nuckolls*^a and Latha Venkataram*^b

Received 16th May 2012, Accepted 9th July 2012

DOI: 10.1039/c2cp41578j

We characterize electron transport across Au–molecule–Au junctions of heterogeneous carboxyl and methyl sulfide terminated saturated and conjugated molecules. Low-bias conductance measurements are performed using the scanning tunneling microscopy based break-junction technique in the presence of solvents and at room temperature. For a series of alkanes with 1–4 carbon atoms in the hydrocarbon chain, our results show an exponential decrease in conductance with increasing molecule length characterized by a decay constant of 0.9 ± 0.1 per methylene group. Control measurements in pH 11 solutions and with COOMe terminations suggest that the carboxylic acid group binds through the formation of a COO^- –Au bond. Simultaneous measurements of conductance and force across these junctions yield a rupture force of 0.6 ± 0.1 nN, comparable to that required to rupture a Au–SMe bond. By establishing reliable, *in situ* junction formation, these experiments provide a new approach to probe electronic properties of carboxyl groups at the single molecule level.

The development of molecular-scale electronics requires an understanding of the relationship between the structure and charge transport properties of single molecules.^{1–3} A molecular junction consists of a molecule bound between two electrodes *via* terminal functional groups that provide both the electronic and mechanical links.^{4–7} The measured conductance of the molecule depends not only on the molecular backbone structure, but also on the choices of the electrode metal and the chemical link group. Specifically, the link group directly affects the type and strength of the metal–molecule interaction, in addition to details such as junction structure due to steric effects. Together, the backbone and the linking groups control both the junction mechanics as well as the electronic level alignment between the metal and the molecule.^{8,9} Many different chemical links have been used experimentally for attaching molecules to Au electrodes including thiols,^{5,8,10,11} amines,^{12–14} methyl sulfides,^{6,15} fullerenes,¹⁶ paracyclophanes,¹⁷ phosphines,^{6,18} cyanides,¹⁹ and covalent gold–carbon links.^{20,21} The links dictate the metal–molecule contact geometry, whose variation can result in significant changes in conductance from junction to junction, particularly if thiol links are used.^{11,22,23} Although electronic measurements of alkanes terminated with carboxylic acid groups have been carried out,¹³ electronic and mechanical properties of conjugated systems have not been reported so far,

despite the attractive chemical modification opportunities afforded by the COOH group.^{24,25} In part, this can be attributed to the practical challenges arising from the low solubility of dicarboxylic acids in most non-polar organic solvents as well as non-trivial adsorption behavior on gold surfaces.³

Here, we overcome these challenges by studying compounds with one carboxylic link and one methyl sulfide (SMe) link; the SMe group has reliable molecular junction formation properties.^{6,15} We measure electronic and mechanical properties of saturated and conjugated molecules terminated with both COOH and SMe linkers. Through conductance measurements across Au–molecule–Au junctions, we find that both SMe and COOH terminations are comparable in terms of their electronics. In addition, we find evidence of binding of the COOH group to gold through a carboxylate–gold (COO^- –Au) bond. Using an atomic force microscope, we also carry out single-molecule bond rupture measurements.^{26,27} We find that these asymmetrically terminated molecular junctions rupture at 0.6 ± 0.1 nN. This force is comparable to the bond rupture force of di-SMe terminated molecules,^{27,28} which indicates that the bond between the acid group and gold electrodes is also mechanically comparable to the Au–SMe bond.

The molecules used in this study, (methylthio)acetic acid (**A1**) (Aldrich), 3-(methylthio)propionic acid (**A2**) (Alfa Aesar), 4-(methylsulfanyl)butanoic acid (**A3**) (Ryan Scientific), 4-(methylsulfanyl)pentanoic acid (**A4**) (Ryan Scientific), and 4-(methylthio)benzoic acid (**B1**) (Aldrich), were purchased and used without further purification. 1,4-bis(methylthio)benzene (**B2**) was synthesized using the procedure of Engman *et al.*^{29,30}

^a Department of Chemistry, Columbia University, New York, NY, USA. E-mail: cn37@columbia.edu

^b Department of Applied Physics and Applied Mathematics, Columbia University, New York, NY, USA. E-mail: lv2117@columbia.edu

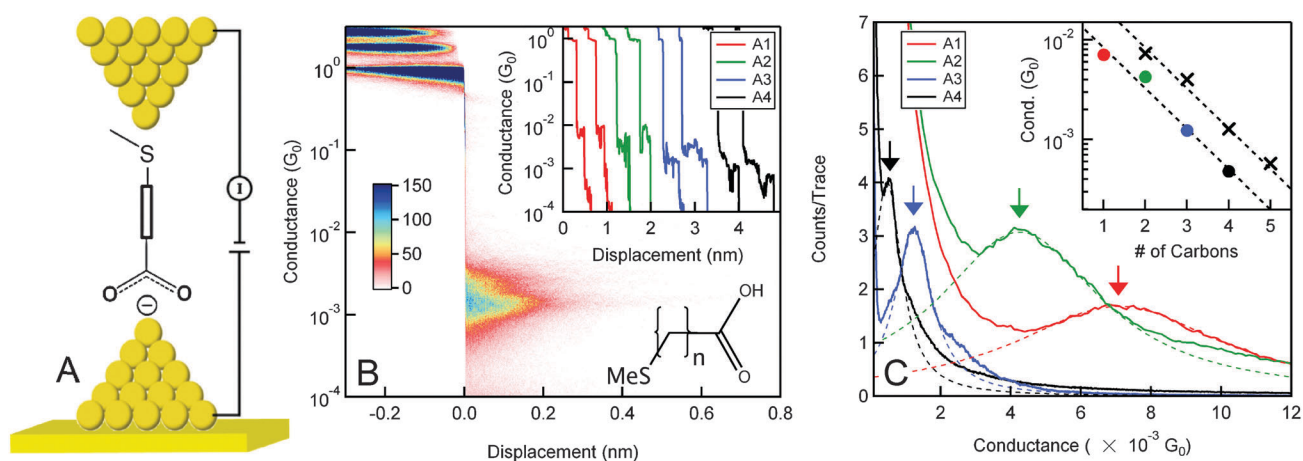


Fig. 1 (A) Schematic illustration of the Au–molecule–Au junction. (B) A 2D conductance–displacement histogram compiled from over 10 000 individual A3 traces measured at a bias of 450 mV. Inset: sample conductance traces of molecules A1–A4. (C) 1D conductance histograms (linear bins, bin-size of $10^{-4} G_0$ for A1 and A2, and $10^{-5} G_0$ for A3 and A4). Inset: semi-logarithmic plot of the variation of the most frequently measured conductance with the number of carbon atoms in the molecule (\bullet = SME–COOH linkers, \times = SME–SMe linkers).

Methyl 4-(methylthio)benzoate (**B3**) was synthesized from 4-(methylthio)benzoic acid using the procedure of Ikeda *et al.*³¹

Molecular conductance measurements are carried out using a modified scanning tunneling microscope⁵ in which a gold tip (cleaved Au wire, 0.25 mm diameter, 99.998%, Alfa Aesar) and a gold coated mica substrate are brought in and out of contact in a 0.1 to 1 mM tetradecane solution of the target molecule (Fig. 1A). The current between the tip and substrate is measured at an applied bias of 450 mV as a function of the relative tip–sample displacement to yield a conductance (current/voltage) *versus* displacement trace. When a clean Au contact is pulled and broken, the conductance traces show steps at integral multiples of G_0 ($G_0 = 2e^2/h$, the quantum of conductance), indicating that the cross-section of the contact is reduced down to that of a few and, eventually, a single atomic chain of Au.³² When the Au single atom chain is broken in the absence of molecules, the conductance either decreases exponentially with the electrode displacement due to tunneling across the gap between the two Au electrodes, or it drops from G_0 to below our experimental detection limit due to the broken ends of the electrode snapping back as the contacts relax.^{33,34} When measurements are carried out with a series of alkanes with 1–4 methylene groups terminated by a COOH group and a SMe group (A1–A4), conductance traces show additional plateaus at characteristic values lower than $1 G_0$ (see Fig. 1B inset). These plateaus are seen if the molecules present in the solution bridge the gap between the electrodes, with the terminal groups forming a bond to the Au electrodes, as illustrated in Fig. 1A.

Fig. 1B shows a two-dimensional conductance histogram^{16,35} created from 10 000 measurements with A3, where all traces are aligned along the displacement axis at the point where the single Au atom contact breaks. We see clear peaks at negative displacements with a conductance around 1, 2 and 3 G_0 , characteristic of Au quantum point contacts. In addition, at positive displacements, we see a distinct conductance signature at around $10^{-3} G_0$ indicating that molecular junctions are formed immediately following the rupture of the Au single-atom contact. This two-dimensional histogram also shows that these molecular

conductance features extend to about 0.2 nm, in good agreement with previous measurements of alkanes terminated with amine or methyl sulfide groups.³⁴ The well-defined distribution of the conductance plateaus indicates that the carboxylic group binds selectively to under-coordinated Au atoms, analogous to amine and methyl sulfide groups.^{6,12} These results together demonstrate that stable single molecule junctions can be reliably formed *in situ* using carboxylic acid linkages.

The variation of conductance with the length of the molecule can reveal information about the electronic structure of the junction.^{2,36,37} We quantify the trends in conductance systematically as a function of the number of methylene groups in the backbone by creating one-dimensional conductance histograms of all measured traces for each compound (Fig. 1C). By fitting the molecular conductance feature in these histograms to a Lorentzian function, we determine the location of the peak in these histograms for each molecule. The peak positions correspond to the most frequently measured conductance of the respective molecule, and are observed to decrease with increasing molecular backbone length. These conductance values are plotted on a semi-logarithmic scale against the number of carbon atoms in each molecule in the inset of Fig. 1C. We note that the number of carbon atoms counted does not include the carbon atom in the COOH group, therefore $n = 1$ for A1 and so on. From a linear fit to these data, we find that the conductance for this series decreases exponentially with increasing molecular length ($G = R_c^{-1}e^{-\beta n}$), where G is the conductance, R_c is the contact resistance, n is the number of carbon atoms in the chain and β is the decay constant. We obtain a decay constant, β , of 0.9 ± 0.1 per methylene group in good agreement with past measurements on a series of alkane molecules with a variety of terminal groups.^{5,6,11,13,38,39} The contact resistance (obtained by extrapolating this fit to zero carbon atoms) is 600 k Ω . For comparison, we include conductance values determined from measurements of alkanes terminated with SMe groups on both ends (\times , inset of Fig. 1C).⁶ Interestingly, we find that the conductance and conductance decay constant of this An series are almost the same as that of the SME-(CH₂)_n-SMe

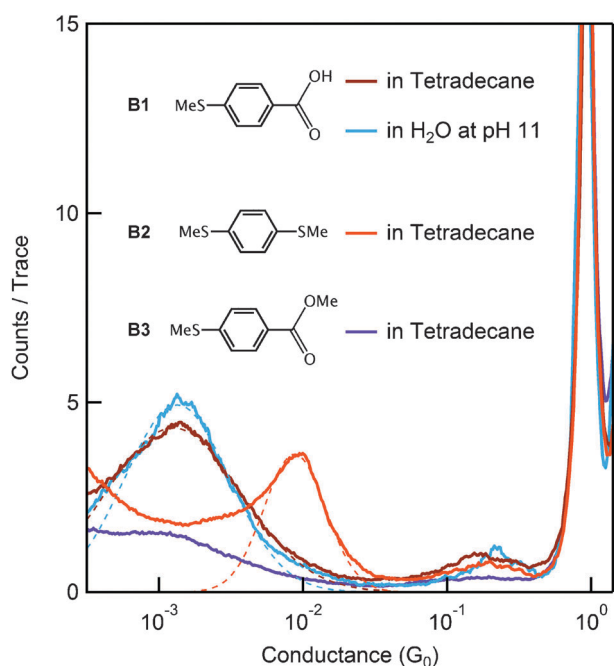


Fig. 2 1D conductance histograms (logarithmic bins, 100 bins per decade) of **B1** in tetradecane (brown) and in water at pH 11 (light blue), and of **B2** (orange) and **B3** (violet) in tetradecane. Measurements were carried out at an applied bias of 450 mV.

compounds (which have a decay constant of 0.9 ± 0.1 per methylene) if we consider that the **An** series has an extra carbon atom within the linker which does not participate in the bonding. Based on this consideration, the contact resistance of the bonding group becomes $240 \text{ k}\Omega$ ($\sim 600 \times e^{-0.9} \text{ k}\Omega$), where the contact resistance of $\text{SMe}-(\text{CH}_2)_n\text{-SMe}$ molecules is $270 \text{ k}\Omega$.⁶ From this, we infer that the electronic coupling between a COOH group and the Au electrode is similar to that of the SMe-Au linkage.

Having established the reliable formation of molecular junctions with COOH linked alkane molecules, we now turn to aromatic systems that have long been known for enhanced electron transfer through solution-based experiments and Marcus-type electron transfer models.⁴⁰ We focus on the prototypical conjugated molecule, 4-(methylthio)benzoic acid (**B1**), with SMe and COOH links on opposite ends and measured in a tetradecane solution. The conductance histogram, generated using logarithmic bins, is shown in Fig. 2 (brown trace). We see a broad molecular conductance feature, indicating that the conductance of **B1** changes from junction to junction, and could depend on the orientation of the molecule in the junction.³⁰ Crucially, we find that the most frequently measured conductance for **B1** is $3\times$ higher than the saturated **A4** molecule, despite their comparable S-S distance. This enhanced conductance clearly demonstrates the more efficient electron transport through the delocalized π -system, at the single molecule level. However, in comparison to its symmetrically linked analogue, **B2** (orange trace in Fig. 2), we note that the conductance of **B1** is smaller, indicating perhaps a reduced coupling due to the additional C atom between the phenyl ring and the Au electrode.

We exploit the chemical modifications afforded by the carboxyl group to probe the binding mechanism between the acid group and the Au electrode. First, we perform the experiment

in the presence of water at a pH of 11 (NaOH base). An apiezon wax coated Au tip is used to minimize the ionic current between the tip and the substrate in the presence of the basic solution.⁴¹ At pH 11, we see the clear molecular conductance feature at the same location ($\sim 1.3 \times 10^{-3} G_0$) as the experiments performed in tetradecane (light blue trace in Fig. 2). Considering the acidic nature of **B1** ($\text{p}K_a = 4.28$), we expect the carboxyl group to be completely deprotonated at pH 11. Therefore, the absence of any changes in the conductance signature indicates that the molecule binds to the electrode through a $\text{COO}^- \text{-Au}$ bond.^{13,42} We also perform the experiment in an acidic solution (pH 1–3), but no identifiable conductance signature is observed. This could be due to the reduced solubility of **B1** in the strongly acidic solution or due to the fact that **B1** is not deprotonated in the low pH solution. To determine if the deprotonation is indeed necessary for bond formation, we perform conductance measurements of methyl 4-(methylthio)benzoate (**B3**), where the hydrogen of the carboxylic group is replaced with a methyl group. As indicated in Fig. 2 (violet trace), we do not observe a clear conductance feature with **B3**. These measurements therefore indicate that the immobilized methyl group blocks the formation of molecular junctions, giving conclusive evidence for a $\text{COO}^- \text{-Au}$ binding mechanism. In addition, this result supports a binding mechanism based on the $\text{COO}^- \text{-Au}$ bond through the negatively charged oxygen atoms, rather than C-Au interactions. This also provides the reason why the carbon atom of the carboxyl group appears to act like an additional atom in the tunneling equation for the alkane series, as discussed above.

In order to test the bond strength between **B1** and Au electrodes, we carry out simultaneous conductance and force measurements on single-molecule junctions following methods previously described by Frei *et al.*²⁶ Briefly, we use a custom-built conductive atomic force microscope (AFM) and form single-molecule junctions between a gold-coated commercial AFM cantilever (NanoAndMore Inc.) and a gold-on-mica substrate. Conductance is measured across the tip-sample junction at a constant bias of 75 mV. The force is measured simultaneously by monitoring the deflection of a laser focused on the back of the cantilever. Fig. 3A displays a sample conductance trace measured in a 1 mM tetradecane solution of **B1**, where we see the characteristic conductance plateau around $\sim 10^{-3} G_0$. Fig. 3B reveals the simultaneously-measured force trace having a characteristic saw tooth pattern that is attributed to reversible (elastic) and irreversible (plastic) deformations during conductance plateaus and drops.⁴³ The conductance and force trace shown in the insets of Fig. 3 have been offset along the displacement axis so that the end of the molecular conductance plateau occurs at zero displacement.

To determine, with statistical significance, the single-molecule junction rupture force, we collect thousands of simultaneous conductance and force traces and analyze this data by using a two-dimensional histogram technique, detailed previously.²⁶ Briefly, the conductance traces are analyzed to select those that have a conductance plateau within the conductance range determined from the histogram shown in Fig. 2, and by requiring a conductance drop of a factor of 5 immediately following the plateau. Although the molecular conductance features are easily recognizable, the short length of **B1** molecule

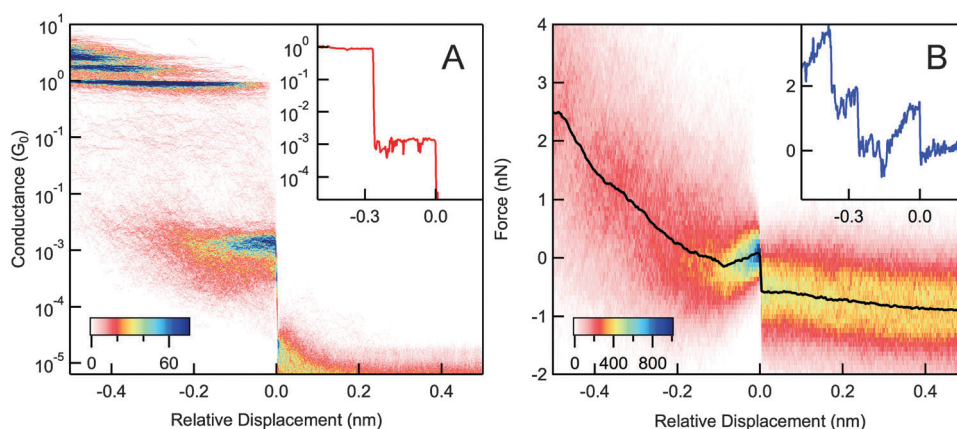


Fig. 3 (A) 2D conductance-displacement histogram of **BI** measured in the conducting AFM setup. Inset: sample conductance trace, offset such that the drop from the molecular conductance plateau occurs at zero displacement. (B) 2D force-displacement histogram constructed from simultaneously measured force across **BI** junctions. The statistically averaged force profile (black line) is overlaid. Inset: sample force trace, measured simultaneously with the conductance trace shown in the inset of Fig. 3A.

results in a relatively infrequent ($\sim 8\%$) formation of single-molecule junctions. These selected conductance traces and the simultaneously measured force traces are then overlaid after aligning each to a common point along the displacement axis (as shown in insets of Fig. 3A and B). All force traces are also aligned along the force axis by adding a constant offset to the entire trace such that the force at the end of the conductance plateau is zero. Fig. 3A and B show the 2D conductance and force histograms, respectively, presenting the statistical representation of all the selected traces. A statistically averaged rupture force is then determined from the profile of the two-dimensional force histogram (black overlaid trace in Fig. 3B). The magnitude of the sharp drop in this profile at zero-displacement corresponds to the average bond rupture force. For measurements with clean gold, we have shown that the rupture force of a gold single-atomic junction is 1.4 ± 0.2 nN. Applying the same methodology to Au-**BI**-Au junctions, we obtain a rupture force of 0.6 ± 0.1 nN. This force is comparable to that required to rupture the Au-NH₂ and Au-SMe bonds,^{26,27} indicating that the COO⁻-Au binding strength is not very different from that of the SMe-Au donor-acceptor bond.

In conclusion, we have experimentally probed the electronic transport through saturated and conjugated molecules with carboxyl linkages. We have shown that the carboxylic acid linker forms mechanically stable single-molecule junction, with a rupture force similar to other well-characterized linkers.^{26–28} Just as in the case of thiol linkers (SH), the hydrogen in the COOH linkers plays a critical role in its binding mechanism to Au electrodes. Taken together, these measurements establish the possibility of using COOH as a mechanically stable and electronically conducting linker group, and open up interesting avenues to a broad range of chemical modifications to tune interfacial electron transfer.

Acknowledgements

This work has been supported in part by the NSF Career Award (CHE-07-44185) and the Packard Foundation. This research was also funded by the National Science Foundation Center for Chemical Innovation (CCI Phase 1 – Award Number CHE-09-43957).

References

- 1 C. Joachim and M. A. Ratner, *Proc. Natl. Acad. Sci. U. S. A.*, 2005, **102**, 8801–8808.
- 2 A. Nitzan and M. A. Ratner, *Science*, 2003, **300**, 1384–1389.
- 3 W. K. Paik, S. B. Han, W. Shin and Y. S. Kim, *Langmuir*, 2003, **19**, 4211–4216.
- 4 M. A. Reed, C. Zhou, C. J. Muller, T. P. Burgin and J. M. Tour, *Science*, 1997, **278**, 252–254.
- 5 B. Q. Xu and N. J. Tao, *Science*, 2003, **301**, 1221–1223.
- 6 Y. S. Park, A. C. Whalley, M. Kamenetska, M. L. Steigerwald, M. S. Hybertsen, C. Nuckolls and L. Venkataraman, *J. Am. Chem. Soc.*, 2007, **129**, 15768–15769.
- 7 M. Kiguchi, O. Tal, S. Wohlthat, F. Pauly, M. Krieger, D. Djukic, J. C. Cuevas and J. M. van Ruitenbeek, *Phys. Rev. Lett.*, 2008, **101**, 046801.
- 8 V. B. Engelkes, J. M. Beebe and C. D. Frisbie, *J. Am. Chem. Soc.*, 2004, **126**, 14287–14296.
- 9 M. S. Hybertsen, L. Venkataraman, J. E. Klare, A. C. Whalley, M. L. Steigerwald and C. Nuckolls, *J. Phys.: Condens. Matter*, 2008, **20**, 374115.
- 10 E. Lortscher, J. W. Ciszek, J. Tour and H. Riel, *Small*, 2006, **2**, 973–977.
- 11 C. Li, I. Pobelov, T. Wandlowski, A. Bagrets, A. Arnold and F. Evers, *J. Am. Chem. Soc.*, 2008, **130**, 318–326.
- 12 L. Venkataraman, J. E. Klare, I. W. Tam, C. Nuckolls, M. S. Hybertsen and M. L. Steigerwald, *Nano Lett.*, 2006, **6**, 458–462.
- 13 F. Chen, X. L. Li, J. Hihath, Z. F. Huang and N. J. Tao, *J. Am. Chem. Soc.*, 2006, **128**, 15874–15881.
- 14 M. Kiguchi, S. Miura, T. Takahashi, K. Hara, M. Sawamura and K. Murakoshi, *J. Phys. Chem. C*, 2008, **112**, 13349–13352.
- 15 J. S. Meisner, M. Kamenetska, M. Krikorian, M. L. Steigerwald, L. Venkataraman and C. Nuckolls, *Nano Lett.*, 2011, **11**, 1575–1579.
- 16 C. A. Martin, D. Ding, J. K. Sorensen, T. Bjornholm, J. M. van Ruitenbeek and H. S. J. van der Zant, *J. Am. Chem. Soc.*, 2008, **130**, 13198–13199.
- 17 S. T. Schneebeli, M. Kamenetska, Z. Cheng, R. Skouta, R. A. Friesner, L. Venkataraman and R. Breslow, *J. Am. Chem. Soc.*, 2011, **133**, 2136–2139.
- 18 R. Parameswaran, J. R. Widawsky, H. Vazquez, Y. S. Park, B. M. Boardman, C. Nuckolls, M. L. Steigerwald, M. S. Hybertsen and L. Venkataraman, *J. Phys. Chem. Lett.*, 2010, **1**, 2114–2119.
- 19 A. Mishchenko, L. A. Zotti, D. Vonlanthen, M. Burkle, F. Pauly, J. C. Cuevas, M. Mayor and T. Wandlowski, *J. Am. Chem. Soc.*, 2011, **133**, 184–187.
- 20 Z. L. Cheng, R. Skouta, H. Vazquez, J. R. Widawsky, S. Schneebeli, W. Chen, M. S. Hybertsen, R. Breslow and L. Venkataraman, *Nat. Nanotechnol.*, 2011, **6**, 353–357.

- 21 W. Chen, J. R. Widawsky, H. Vázquez, S. T. Schneebeli, M. S. Hybertsen, R. Breslow and L. Venkataraman, *J. Am. Chem. Soc.*, 2011, **133**, 17160–17163.
- 22 J. Ulrich, D. Esrail, W. Pontius, L. Venkataraman, D. Millar and L. H. Doerrer, *J. Phys. Chem. B*, 2006, **110**, 2462–2466.
- 23 X. L. Li, J. He, J. Hihath, B. Q. Xu, S. M. Lindsay and N. J. Tao, *J. Am. Chem. Soc.*, 2006, **128**, 2135–2141.
- 24 H. J. Himmel, K. Weiss, B. Jäger, O. Dannenberger, M. Grunze and C. Wöll, *Langmuir*, 1997, **13**, 4943–4947.
- 25 A. Cossaro, M. Puppini, D. Cvetko, G. Kladnik, A. Verdini, M. Coreno, M. de Simone, L. Floreano and A. Morgante, *J. Phys. Chem. Lett.*, 2011, **2**, 3124–3129.
- 26 M. Frei, S. V. Aradhya, M. Koentopp, M. S. Hybertsen and L. Venkataraman, *Nano Lett.*, 2011, **11**, 1518–1523.
- 27 M. Frei, S. V. Aradhya, M. S. Hybertsen and L. Venkataraman, *J. Am. Chem. Soc.*, 2012, **134**, 4003–4006.
- 28 S. V. Aradhya, J. S. Meisner, M. Krikorian, S. Ahn, R. Parameswaran, M. L. Steigerwald, C. Nuckolls and L. Venkataraman, *Nano Lett.*, 2012, **12**, 1643–1647.
- 29 L. Engman and J. S. E. Hellberg, *J. Organomet. Chem.*, 1985, **296**, 357–366.
- 30 Y. S. Park, J. R. Widawsky, M. Kamenetska, M. L. Steigerwald, M. S. Hybertsen, C. Nuckolls and L. Venkataraman, *J. Am. Chem. Soc.*, 2009, **131**, 10820–10821.
- 31 A. Ikeda, K. Terada, M. Shiotsuki and F. Sanda, *J. Polym. Sci., Part A: Polym. Chem.*, 2011, **49**, 3783–3796.
- 32 H. Ohnishi, Y. Kondo and K. Takayanagi, *Nature*, 1998, **395**, 780–783.
- 33 A. I. Yanson, G. R. Bollinger, H. E. van den Brom, N. Agrait and J. M. van Ruitenbeek, *Nature*, 1998, **395**, 783–785.
- 34 M. Kamenetska, M. Koentopp, A. Whalley, Y. S. Park, M. Steigerwald, C. Nuckolls, M. Hybertsen and L. Venkataraman, *Phys. Rev. Lett.*, 2009, **102**, 126803.
- 35 S. Y. Quek, M. Kamenetska, M. L. Steigerwald, H. J. Choi, S. G. Louie, M. S. Hybertsen, J. B. Neaton and L. Venkataraman, *Nat. Nanotechnol.*, 2009, **4**, 230–234.
- 36 K. Moth-Poulsen and T. Bjornholm, *Nat. Nanotechnol.*, 2009, **4**, 551–556.
- 37 A. Salomon, D. Cahen, S. Lindsay, J. Tomfohr, V. B. Engelkes and C. D. Frisbie, *Adv. Mater.*, 2003, **15**, 1881–1890.
- 38 H. B. Akkerman and B. de Boer, *J. Phys.: Condens. Matter*, 2008, **20**, 013001.
- 39 D. J. Wold, R. Haag, M. A. Rampi and C. D. Frisbie, *J. Phys. Chem. B*, 2002, **106**, 2813–2816.
- 40 J. Halpern and L. E. Orgel, *Discuss. Faraday Soc.*, 1960, **29**, 32–41.
- 41 L. A. Nagahara, T. Thundat and S. M. Lindsay, *Rev. Sci. Instrum.*, 1989, **60**, 3128–3130.
- 42 W.-k. Paik, S. Han, W. Shin and Y. Kim, *Langmuir*, 2003, **19**, 4211–4216.
- 43 P. E. Marszalek, W. J. Greenleaf, H. B. Li, A. F. Oberhauser and J. M. Fernandez, *Proc. Natl. Acad. Sci. U. S. A.*, 2000, **97**, 6282–6286.